Available online at www.sciencedirect.com
SCIENCE DIRECT
Polymer 46 (2005) 11582–11590
polymer
www.elsevier.com/locate/polymer

Syndiotactic polypropylene as potential material for the preparation of porous membranes via thermally induced phase separation (TIPS) process

Wilfredo Yave[a,*], Raúl Quijada[a], Mathias Ulbricht[b], Rosario Benavente[c]

[a]*Departamento de Ingeniería Química, Facultad de Ciencias Físicas y Matemáticas, Universidad de Chile, y Centro para la Investigación Interdisciplinaria Avanzada en Ciencia de los Materiales (CIMAT), Santiago, Chile*
[b]*Lehrstuhl für Technische Chemie II, Universität Duisburg-Essen, Essen, Germany*
[c]*Instituto de Ciencia y Tecnología de Polímeros (CSIC), Madrid, Spain*

Received 8 June 2005; received in revised form 30 September 2005; accepted 1 October 2005
Available online 24 October 2005

Abstract

This work reports the flat sheet membrane preparation from syndiotactic polypropylene (sPP) by thermally induced phase separation (TIPS) process. sPP obtained by polymerization using metallocene catalysts and isotactic polypropylene (iPP) also obtained via metallocene catalysis with similar molecular weight were used. The phase diagrams of sPP and iPP with diphenylether as diluent were obtained. The properties of three representative membranes from sPP and three from iPP, prepared using different PP concentrations were evaluated with respect to membrane pore structure, gas flow, liquid displacement (bubble point), and water permeability. Two selected membranes, one from sPP and one from iPP were analysed with regard to polypropylene bulk morphology (X-ray diffraction) and mechanical properties (tensile strength). Under the same formation conditions, membranes with less inter-connected pores and less porous surface were obtained from sPP compared with iPP. Overall, lower permeabilities had been found for the sPP membranes, which were attributed to the difference in pore morphology. The differences between sPP and iPP were also discussed in terms of different driving forces for liquid–liquid demixing as deduced from the phase diagrams. The X-ray analysis had shown that the sPP membranes had a higher amorphous phase content than that in iPP, and the mechanical test had revealed a pronounced ductile behaviour for sPP samples. These results helped to explain the lower permeabilities of the sPP membranes, and their pressure-dependency.

Keywords: Syndiotactic polypropylene; Microfiltration membrane; TIPS process

1. Introduction

Microporous membranes are used in a very wide range of applications, especially in microfiltration. Examples include the removal of bacteria and viruses, the clarification of beer or wine, the treatment of waste water, oil–water separation, the oxygenation or using them as base material for affinity separation [1–5]. Porous membranes from polypropylene are of particular relevance, mainly due to their good mechanical properties, chemical and thermal stability, hydrophobicity, and low cost [6,7]. On the other hand, in the preparation of membranes from polyolefins, thermally induced phase separation (TIPS) process has gained significant attention from both scientific and practical point of view. Several studies about the membrane formation by the TIPS process have been devoted to the mechanisms of phase separation, including the effects of diluents and polymer molecular weight, as well as the concentration and temperatures profiles [8–12].

Recent progress of catalyst technology for olefin polymerization has contributed to the development of new polymeric materials with a wide range of controlled macromolecular structures, such as isotactic, syndiotactic or stereoblock polymers [13–15]. Syndiotactic polypropylene (sPP) with high tacticity and high molecular weight obtained by metallocene catalysts is receiving a great attention owing to its special properties compared to the isotactic polyproylene (iPP) [16–19]. Therefore, new applications could be based on this novel material. As it is well known, sPP has the same constitution as the commonly used iPP, but it has a different stereoregular structure because all methyl groups attached to the macromolecules are alternately arranged with regard to the main chain plane.

In order to elucidate the relationships between polymer microstructure, membrane morphology, and permeability, we

* Corresponding author. Tel.: +56 2 678 4730; fax: +56 2 699 1084.
E-mail address: wyave@ing.uchile.cl (W. Yave).

0032-3861/$ - see front matter © 2005 Elsevier Ltd. All rights reserved.
doi:10.1016/j.polymer.2005.10.012

have started to study the membrane preparation from different polypropylenes obtained by metallocene catalysts. The present work is a study devoted to the preparation and characterization of flat sheet porous membranes from sPP by the TIPS process, based on comparison of the novel sPP with iPP having similar average molecular weight, and the same molecular weight distribution.

2. Experimental part

2.1. Materials

Syndiotactic polypropylene synthesized in our laboratory by metallocene catalysts as described elsewhere [20,21] was used for membrane preparation. In addition, an isotactic polypropylene also prepared via metallocene catalysis was used for comparison. The average molecular weights were $M_w =$ 290 kg/mol for sPP, and 310 kg/mol for iPP, the molecular weight distributions were identical ($M_w/M_n = 1.8$), these properties had been determined using gel permeation chromatography (GPC) with a Waters Alliance GPC2000 system at 408 K. The stereoregularity of the polymers was confirmed through the ^{13}C NMR (nuclear magnetic resonance) spectra at 393 K in a Varian Innova 300 at 75 MHz. The content of 'rr' triad was 62% and the 'mm' triad 93%, respectively. Diphenylether (DPE) from Aldrich was used without further purification as diluent for membrane preparation. The solvents used, methanol and isopropanol (both from Aldrich) were of technical grade.

2.2. Phase diagram

To obtain the phase diagrams, polymer-diluent samples with different concentrations were loaded into capillary tubes, which were then purged with nitrogen, sealed to prevent oxidation, and heated in an electrothermal equipment 9100 (Merck) at 453 K. The cloud point was determined visually by noting the first appearance of turbidity under optical eyeglasses incorporated in the electrothermal equipment. The values obtained are from an arithmetic mean of three measurements.

The melting temperature of the polymer samples and dynamic crystallization temperatures of the polymer in the polymeric solution were determined calorimetrically using a Modulated TA Instruments DSC 290 differential scanning calorimeter (DSC), at a cooling rate of 10 K/min.

2.3. Membrane preparation

The thermally induced phase separation (TIPS) process was used to prepare the flat sheet membranes, this procedure is described in several previous reports [9,22–25]. Briefly, sPP or iPP and DPE (PP nominal concentration at 20, 15 and 13 wt%) were filled in a test tube, which was purged with nitrogen and sealed to prevent the oxidation. The test tube was placed in an oven at 453 K for 12 h to homogenize the solution, and then it was immersed in liquid nitrogen in order to induce the solidification. A small amount of the solid solution was taken and placed on a circular thin film mould with a diameter of 5 cm made from aluminium, and then it was covered with another aluminium thin plate (Fig. 1). The use of two different moulds allowed the preparation of samples with either 500 or 200 μm thickness, approximately. This assembly was heated in the oven at 453 K for 10 min to eliminate the possible influence of the thermal history. Then it was immersed in water at room temperature to induce the phase separation. The loss of DPE during this procedure was experimentally controlled, and it had been found to be <3 wt%, so that the overall PP concentration would increase by <0.6 wt%. Finally, the DPE in the membrane was extracted with methanol in a soxhlet apparatus for 6 h, and then the porous membrane was dried in an oven at 333 K overnight.

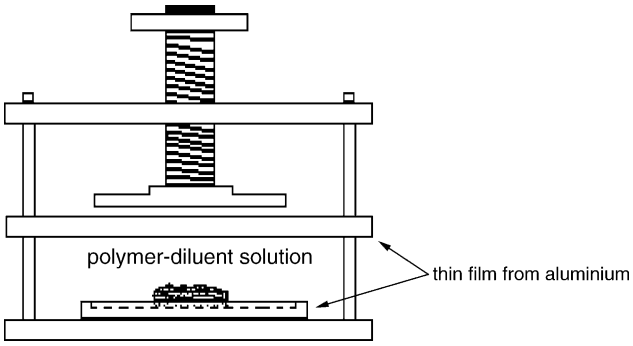

Fig. 1. Flat sheet membrane preparation system.

2.4. Membrane characterization

Attenuated total reflection Fourier transform Infra-red (ATR-FTIR) spectra were recorded using a spectrometer IFS 55 EQUINOX (Bruker), it was equipped with a horizontal ATR unit at a nominal resolution of 4 cm^{-1} and 256 scans. This experiment was used to verify the DPE extraction from the polymer matrix.

The membrane porosity was determined based on gravimetric measurements of the difference between dry and fully solvent-filled samples. Isopropanol was used as solvent ensuring complete wetting of all pores. The following equation was used to calculate the porosity:

$$\text{Porosity} = \frac{(m_w - m_d)}{\rho \pi r^2 e} 100\% \quad (1)$$

where, m_w and m_d are the mass of the wet and dry membrane, respectively, ρ is the isopropanol density (0.798 g/cm^3), r is the membrane sample radius, and e is the membrane thickness.

Membrane pore morphology was examined using a TESLA BS343A scanning electron microscope (SEM) at an accelerating voltage of 15 kV. The samples were fractured in liquid nitrogen, and then sputter-coated with gold in order to examine the membrane cross-section and outer surface.

The analysis of the polypropylene bulk crystallinity in the membranes was based on the wide-angle X-ray diffraction (WAXD) patterns in the reflection mode. A Philips diffractometer with a Geiger counter, connected to a computer, using

Ni-filter Cu K_α radiation was used. The diffraction scans were collected at room temperature over a period of 20 min in the range of 2θ values from 3 to 43° using a sampling rate of 1 Hz. The goniometer was calibrated with a silicon standard.

Gas flow and liquid displacement of a pore-filling liquid (1,1,2,3,3,3-hexafluoro-propene with a surface tension of 16 dyn cm^{-1}) yielding the bubble point pore diameter (d_{bp}) of the membranes (sample area 4.9 cm^2) were measured using a permporometer CFP-34RTG8A-X-6-L4 (PMI, USA).

To calculate the average pore size (r_g), it has been used the Darcy's law, which governs the gas flow through the pores media. Darcy's law in the specific notation of the Hagen–Poiseuille equation can be written as follows:

$$F = \frac{kA}{\mu e}(P_2 - P_1) \tag{2}$$

$$F = \frac{\varepsilon A r_g^2}{8\mu e}(P_2 - P_1) \tag{3}$$

where F, k, A, r_g, ε, μ, e, and P are the volumetric flux, Darcy permeability, cross-sectional area of the membranes, pore mean radius, effective porosity, fluid viscosity, thickness of the membrane, and pressure, respectively.

Water permeability of the membranes (sample area 4.9 cm^2) was measured in a pressure driven filtration cell with a magnetic stirrer (Amicon 8010, Millipore). Before measuring the water flux, the membranes were carefully wetted with isopropanol followed by water.

The mechanical properties of the membranes were evaluated in a stress–strain test using an Instron Universal testing machine (Instron), calibrated according to standard procedures and equipped with a load cell and an integrated digital display that provided force determination. A load of 100 N and a strain rate of 0.67 min^{-1} were used. The samples had 2.5 mm of width and the distance between the gags was 10 mm.

3. Results and discussion

3.1. Phase diagrams and membrane preparation

The phase diagrams for both sPP-DPE and iPP-DPE systems are shown in Fig. 2. A binodal curve, a liquid–liquid phase (below the binodal curve), a solid–liquid phase (at PP concentration higher than 50 wt%), a dynamic crystallization curve, and a monotectic point (intersection between binodal and crystallization curve) can be distinguished.

A shift of the binodal curve (connected points) to higher temperature, and a shift of the dynamic crystallization curve to lower temperature in the sPP-DPE system compared to the iPP-DPE system were observed, and these results could lead to a different final morphology and different properties in the membranes. The influence of the sPP microstructure on the phase diagram and pore growth have been widely analysed and discussed in a previous report [25]. Briefly, the shift of the

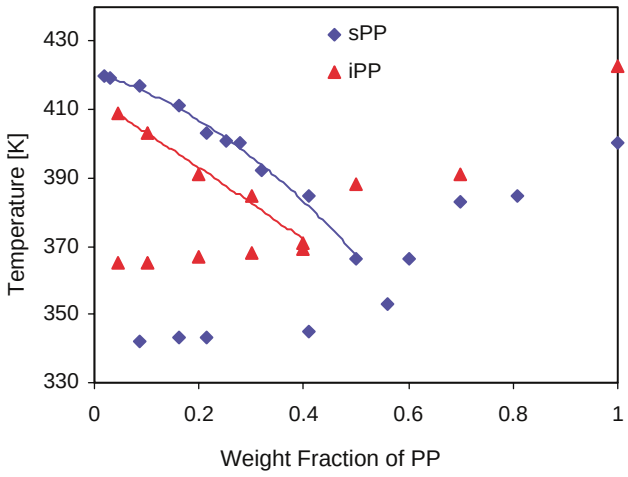

Fig. 2. Phase diagrams for sPP-DPE and iPP-DPE systems (interconnected points are bimodal curve, and not interconnected points are on the dynamic crystallization line).

bimodal curve was attributed to stereochemistry effects, chain rigidity and local chain packing of the sPP, and the pore growth was influenced by difference in viscosity and growth period in each system.

In order to achieve a good reproducibility of the membrane preparation, several series of preliminary experiments in each condition had been made. Once those conditions had been established, the PP concentrations have been selected inside the liquid–liquid region of the phase diagram. This selection was done to obtain a porous membrane structure. In particular, rather low polymer concentrations have been studied in order to obtain membranes with high porosity. Based on similar considerations, the quenching temperature difference from 453 K to room temperature has been selected. Two constant initial film thicknesses (200–500 μm) were used; the design and the material of the mould should be suited to prepare membranes with isotropic structure [23,26]. However, the temperature gradients through the film thickness could lead to some anisotropy [7,23,27], and thus it could not be excluded to priori. An overview of the different membranes is given in Table 1. As membrane preparation was made after having achieved good reproducibility, the thickness and the porosity error was found in ±5% approximately. The samples shown in Table 1 had been selected because the full set of morphology, permeability and other data had been collected for these particular membranes. In the preliminary experiments it had been confirmed that those samples are representative for the materials obtained as a function of the varied membrane polymer and polymer concentrations.

As it is known, the membrane preparation by the TIPS process is from a biphasic polymer-diluent system, thus the resulting membrane consists of a polymeric matrix and pores filled with diluent. Therefore, for the characterization and final application, the membranes should be free of diluent.

Fig. 3 shows ATR-FTIR spectra for two selected samples of iPP and sPP membranes prepared from 14.0 to 13.5 wt% polymer solution, respectively. This spectrum allows verifying

Table 1
Properties of the membranes obtained by the TIPS process

Sample	PP concentration [wt%]	Thickness [μm]	Porosity [%]	$k\times10^4$[cm^2][a]	$2\times r_g$ [μm]	d_{bp}[μm]
sPP	20.0	550	61	0.98	0.1	0.4
	15.0	450	60	13.01	0.3	0.9
	13.5	650	77	45.08	0.4	2.5
iPP	19.0	150	52	4.09	0.2	1.0
	15.0	200	65	29.75	0.4	1.5
	14.0	600	77	60.20	0.5	1.9

[a] Darcy permeability.

that the DPE has been extracted completely from the polymer matrix. As is evident, the characteristic absorption bands for sPP and iPP also appear in iPP-DPE sample, except for the intense bands between 600 and 1700 cm^{-1}. These would correspond mainly to DPE, and thus, this result could be interpreted as sensitive to DPE extraction.

3.2. Membrane pore structure

The overall membrane porosities can be seen in Table 1. The porosity increased when the initial concentration of polymer-diluent solution decreased, only the sPP membrane prepared from 15 wt% of polymer concentration was an exception.

Figs. 4 and 5 show the outer surface morphologies and cross sections of the different membranes prepared from sPP and iPP. These morphologies indicate that the pore structures were formed by liquid–liquid phase separation [9,28,29]. In those micrographs for both polymer membranes, the characteristic pore size increased systematically with decreasing PP concentration. On the other hand, the morphologies in the iPP membranes prepared from 19 to 15 wt% polymer solution having a thinner thickness than all the other membranes did not show special features, e.g. the pore size was increased (cf. below). Thus, it would indicate that there was not an effect of the thickness onto membrane structure.

Overall, the internal pore diameter could be estimated, being between 1 and ~10 μm. However, marked differences have been seen for the outer surfaces: the iPP membranes had a much larger surface porosity than the sPP membranes, and for both polymers the surface porosity also is increased with decreasing of the PP concentration, especially for the sPP membranes prepared using the highest PP concentration (20 wt% in polymer), hardly any pore could be detected on the outer surface.

It is well know, that in the TIPS process, two factors contribute to the final pore structure [23–31]: pore growth rate and growth period. The growth rate depends mainly on the viscosity of the polymer system, while the growth period depends on the cooling rate and the temperature difference between binodal and crystallization curves in the phase diagram. The cooling rate was the same for all experiments, but the difference between binodal and crystallization curves is greater for the sPP-DPE system than for that in iPP-DPE (cf. Fig. 2). This temperature difference should allow having larger pores in sPP sample than iPP. However, the results observed in the SEM micrographs did not confirm this assumption. As it is shown and discussed elsewhere [25], the iPP-DPE had a lower viscosity than the sPP-DPE system, which would allow a faster pore growth in iPP, leading to larger and more interconnected pores in the iPP membranes than sPP.

The increase of pore size with decreasing initial PP concentration could also be explained by the increase of the temperature difference between binodal and crystallization curves in the phase diagram (cf. Fig. 2), allowing a longer time for growth of the pores [32,33]. At the same time, the viscosity will also decrease, and thus, both effects could synergistically lead to larger pores in the iPP systems.

On the other hand, sPP membranes have presented different surface structure compared to iPP. Figs. 4 and 5 suggest that the iPP membranes have a larger surface roughness than the sPP membranes. Several recent studies had revealed that an increase of the hydrophobicity can result from an increase of the surface roughness in the lowest micrometer range, so that the contact area between water and the solid surface would be minimized [34]. This difference in roughness is also important to explain the difference in permeability of the membranes, which will be shown later on.

The main reasons for the differences in membrane morphology could be related to the sPP and iPP

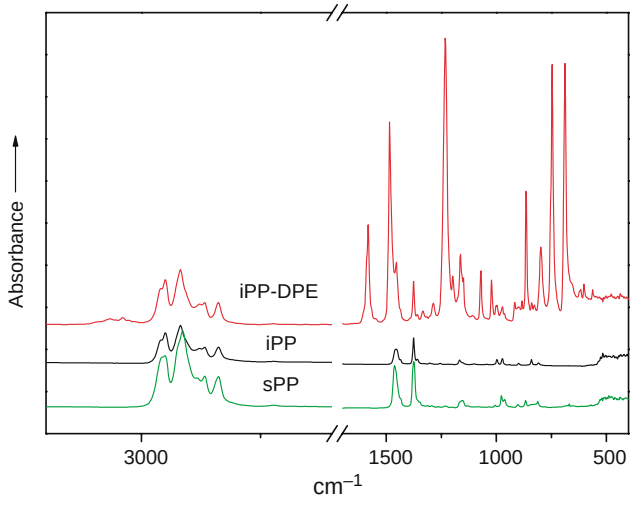

Fig. 3. ATR-FTIR spectra of the iPP-DPE sample (before of the DPE extraction), iPP and sPP membranes after of the DPE extraction.

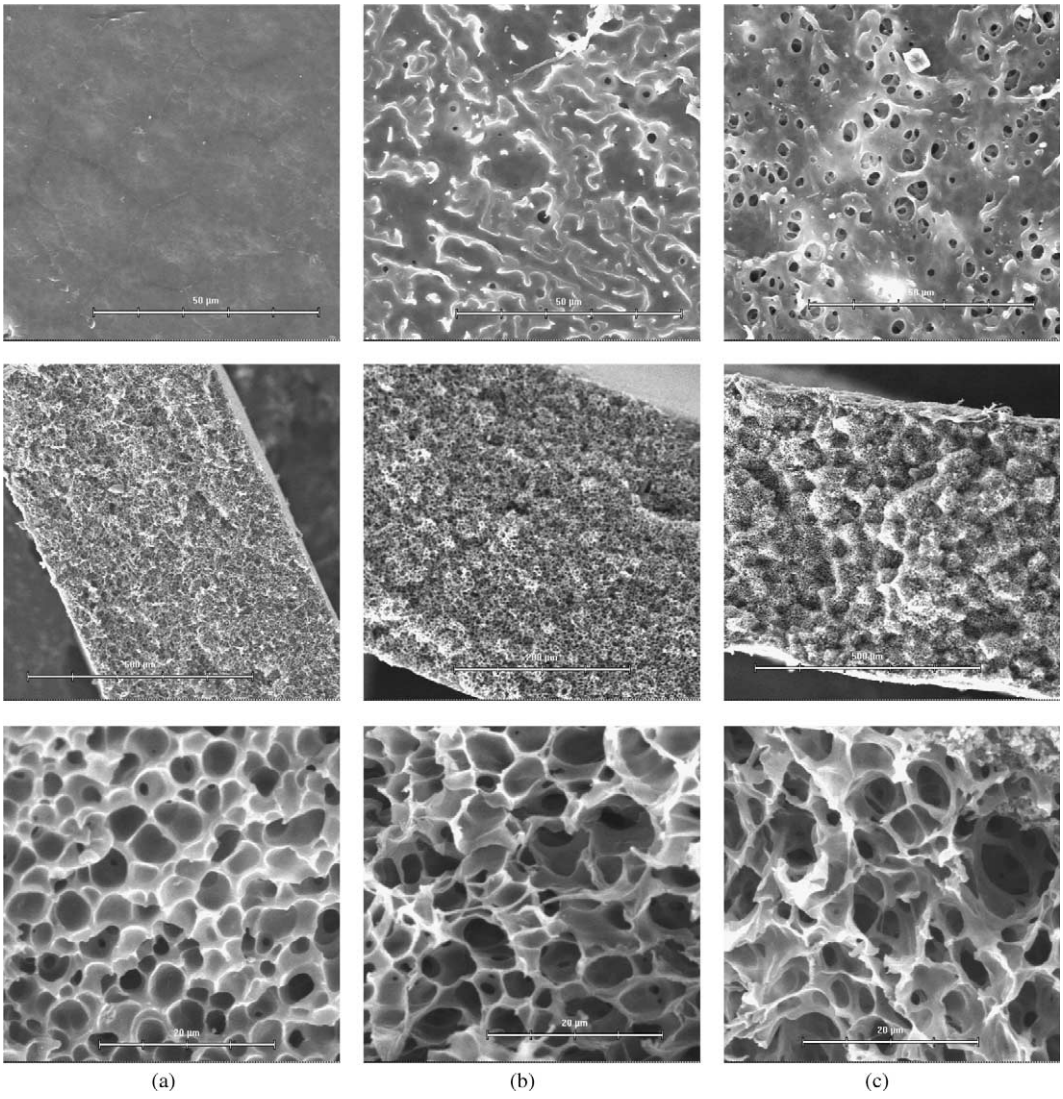

Fig. 4. Final morphology of the outer surface and the cross section (overview and detail from the inner part of the structure) of the sPP membranes: (a) 20 wt%, (b) 15 wt%, and (c) 13.5 wt%.

microstructures and consequently to their properties, just as it was shown in previous report [25]. Both, polymer concentration gradients due to solvent evaporation before closing the system [23,26], which had been found to be $<0.3\%$; (cf. experimental part) and cooling rate gradients (due polymer film thickness) could induce an anisotropic membrane pore structure near to the membrane surface, since cooling rate in the surface is faster than inside the membrane [35,36], but those factors would be present for both systems. As membrane preparation was made in a mould during the membrane formation, the interfaces between polymer solution and aluminium may have an influence, since some of the chemical and physical properties are significantly different for iPP and sPP. Examples for such differences can be seen in melting temperature (cf. Fig. 2) and degree of crystallinity (cf. Fig. 6). The mould surface had not been modified in order to not change the wetting properties of the membrane surface; a study could provide more insights into possible reasons for the different morphologies of the outer surfaces.

3.3. Polypropylene bulk morphology

Fig. 6 displays the wide angle X-ray diffraction (WAXD) patterns for two selected membranes from iPP and sPP (obtained from a solution at 14–13.5 %wt in PP, respectively). In addition, a corresponding pattern for amorphous PP component is presented.

The porous membrane from iPP exhibits the five main diffractions, corresponding to the (110), (040), (130), (111) and (041, 131) reflections characteristic of the monoclinic α modification of iPP (no indication of γ modification is detected) [37,38].

However, the porous membrane from sPP exhibits exclusively four main diffractions at 2θ values of 12.2, 15.8, 20.6 and 24.6 corresponding to (200), (010), (111) and (400) reflections characteristic of the disordered Form I [38–43]. The absence of the 211 reflection at $2\theta = 18.8^\circ$ confirms that the disordered Form I had been obtained. The preferential crystallization in this Form I had been usually found in

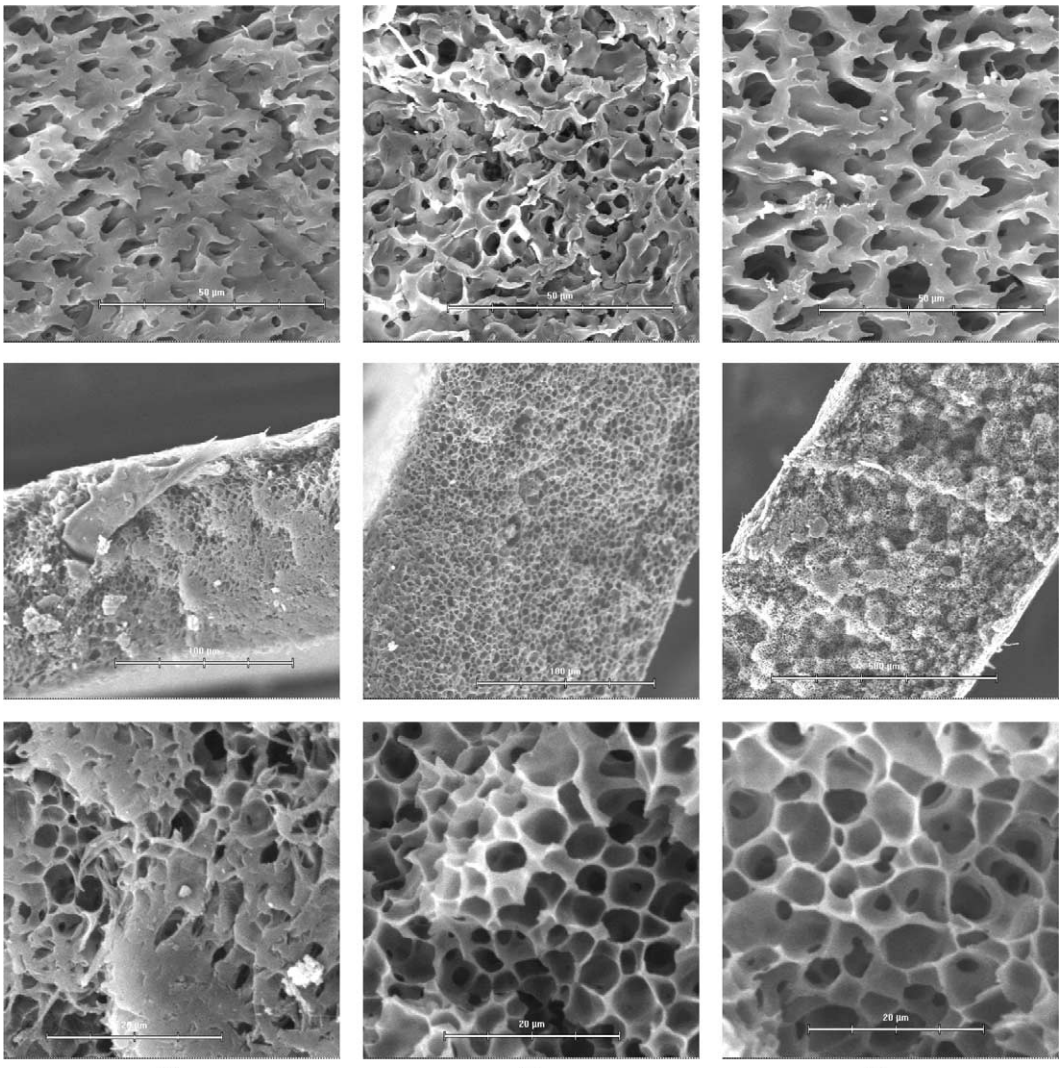

Fig. 5. Final morphology of the outer surface and the cross section (overview and detail from the inner part of the structure) of the iPP membranes: (a) 19 wt%, (b) 15 wt%, and (c) 14 wt%.

samples with low syndiotacticity and/or samples crystallized at low temperature [44].

The degree of crystallinity from X-ray diffractograms for iPP and sPP was assessed by subtracting the corresponding pattern of the amorphous component. In this case we have used a totally amorphous atactic polypropylene [45], and the resulting values are presented in Table 2. Hence, significantly different mechanical properties would be expected, e.g. a more ductile behaviour of the sPP membranes.

The large difference in the degree of crystallinity between sPP and iPP samples was evident, and together with the difference in microstructure it would have affected to the polymer-diluent phase diagram. Therefore, the difference between membrane morphologies obtained from these systems, especially the pore size of the membrane from sPP, may be highly influenced by these physical characteristics of the polymer [46]. In addition, the sPP is more amorphous than iPP (Table 2), thus the iPP would provide more stability to the

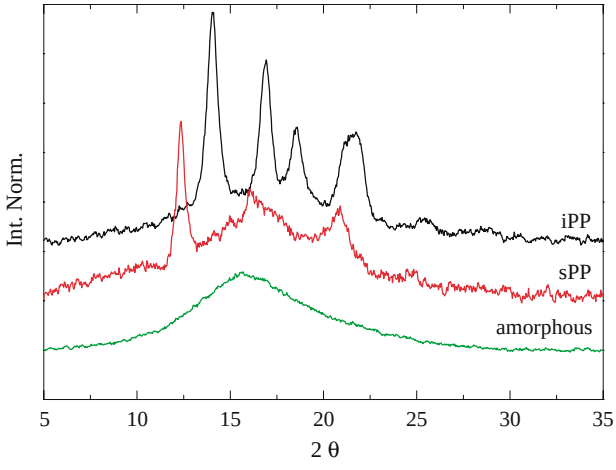

Fig. 6. X-ray diffraction patterns of selected iPP and sPP membranes, and amorphous PP sample.

Table 2
Crystallinity and main mechanical properties of the two selected membranes

Samples	Crystallinity [%]	E [MPa]	σ_y [MPa]	ε_B [%]
iPP	60	35	2.0	150
sPP	35	27	1.5	400

cellular structure during the extraction and drying stages that are used to prepare the membrane for SEM characterization.

3.4. Gas permeability and wetting liquid displacement

Gas permeability test is often applied to characterize the integrity of a membrane, but may also provide information about the pore structure. For all membranes, the nitrogen permeability increased linearly with the rise in transmembrane pressure. This linear behavior could be attributed to a laminar flow and would obey the Darcy's law in the specific notation of the Hagen–Poiseuille equation [47,48]. Gas permeability has been expressed in terms of the Darcy permeability (k) (cf. Table 1), and the pore mean radius (r_g) of the membrane could be estimated from it. Due to the significant deviations from cylindrical pore geometry, these data may only provide a very rough approximation, but nevertheless, the differences in pore structure could be quantified. Furthermore, the bubble point pore diameter (d_{bp}) has been obtained from liquid displacement (cf. Table 1). Note, however, that d_{bp} will only indicate the size of the largest pore acting as transmembrane barrier while the pore mean radius is representative for the entire pore size distribution. It should be noted that the values determined from the gas permeability experiments were obtained considering the differences in membranes thickness.

The permeabilities (k) for iPP membranes were higher than those for the sPP membranes, both prepared from the same PP initial concentration. These differences were especially large for the membranes prepared from the highest PP concentration (20 wt%). Hence, the average pore size in sPP membranes was slightly smaller than in the corresponding iPP membranes. A similar tendency, with a deviation for the sPP membrane prepared from the highest PP concentration, has been seen for the bubble point pore diameter.

Considering the large difference between volume and surface pore structure of the membranes seen in SEM analysis (Figs. 4 and 5), the differences in the absolute values between pore mean diameter and bubble point pore diameter can be well understood.

3.5. Water permeability

The water permeability is a most important performance criterion for microfiltration membranes. The data for all membranes at different transmembrane pressures are shown in Fig. 7, the permeability values in these figures are the average of a series of samples prepared in the same conditions.

In these plots, is clearly observed that the water permeability of both sPP and iPP membranes increased when the PP concentration was reduced (cf. Table 1). As discussed above, these results can be related to an increase of the pore sizes and porosities, which were related with the temperature difference between binodal and crystallization curve in the phase diagram (cf. Fig. 2).

However, a closer inspection of the water permeability data reveals that for the sPP membranes, but not for the iPP membranes, the permeability decreased with increasing transmembrane pressure. An important factor related to the permeability of the sPP membranes may be the compression of the pores during the microfiltration process. This effect can be related to the ductile behavior of sPP which will be shown in the next section, and this is caused by the much lower crystallinity of the sPP than iPP samples (cf. Fig. 6).

3.6. Mechanical properties of the polypropylene membranes

The stress–strain analysis for two selected specimens stretched at 0.67 min^{-1} was carried out. Young modulus (E), yield stress (σ_y) and strain break (ε_B) were determined from those curves, which are summarized in Table 2. The yield stresses were determined by the tangent method [49].

Significant differences were observed. The Young modulus (determined by the slope of the curve) and the yield stress were higher in the iPP than sPP sample, but the strain break was at 150% for iPP and at 400% for sPP. The higher ductile behavior

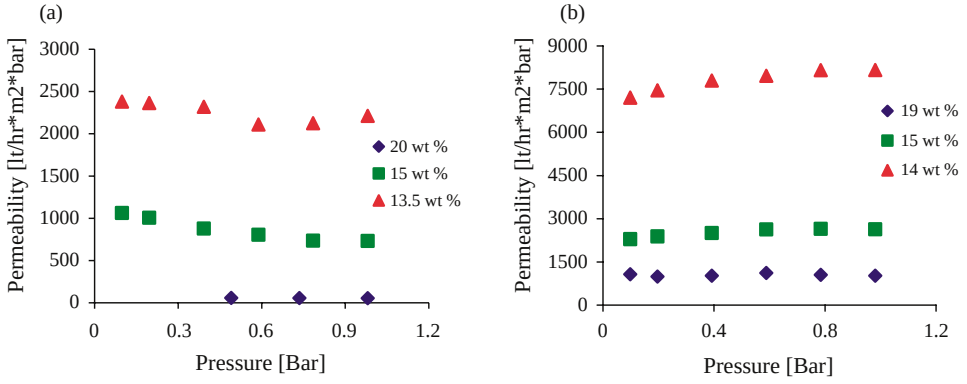

Fig. 7. Water permeability through the membranes: (a) sPP at 20, 15 and 13.5 wt%; and (b) iPP at 19, 15 and 14 wt% polymer nominal concentration used for membrane formation.

of the sPP membranes than iPP would indicate that the polypropylene microstructure affected to the mechanical properties of the membranes, thus it would confirm the pores compression during the microfiltration process.

The behavior of both iPP and sPP can be related with the crystallinity, and it is clearly seen that higher crystallinity gives a larger modulus. However, the absolute values are different to these reported in the literature, because in this case the samples have porosity. While, many studies of the sPP mechanical behavior had confirmed its great flexibility [46,50], no characterizations of porous membranes had been done yet. Therefore, the main factor to explain the difference in absolute values is the presence of pores in the polymer matrix.

4. Conclusions

Polypropylenes obtained via metallocene catalysts had been used to prepare porous membranes by the TIPS process. The dominating membrane formation mechanism was liquid–liquid phase separation. When the initial concentration of the polymer-diluent system was decreased, polypropylene membranes with higher porosity and larger pores have been obtained. This result was related to the larger temperature difference between binodal curve and dynamic crystallization curve in the phase diagram, leading a longer time for the pore growth. However, under the same formation conditions, significantly smaller pore sizes, and presumably, lower connectivity was obtained from sPP. This was mainly attributed to the difference of properties among the polymers and to the higher viscosity of the sPP-DPE solutions compared with the iPP system [25]. In addition, the surface porosities of the sPP membranes were lower than for iPP for each polymer concentration.

The overall lower permeabilities of the sPP membranes had been attributed to the differences in pore structure. However, the lower water permeabilities of sPP have also been related to the compression of the porous structure during pressure-driven filtration, since sPP membranes had more amorphous phase than iPP, and showed a pronounced ductile behavior in stress–strain analysis.

Finally, we can conclude that flat sheet porous membranes from sPP have been obtained for first time, and these novel membranes have been evaluated in terms of their formation conditions as well as the pore structures and permeabilities were related. The ductility and the hydrophobicity of the sPP which had not been used as membrane material yet may be the base for further applications, and this will be investigated in future work.

Acknowledgements

The authors acknowledge the financial support to CONICYT through of the FONDAP-11980002, CSIC/CONICYT 2003CL0028 project and to Ministerio de Educación y Ciencia (Project MAT2004-01547). We also thank the Deutscher Akademischer Austauschdienst (DAAD) for the PhD scholarship, and a short-time y Postitulo de la Universidad de Chile, Beca (PG/68/2004). Finally, we are indebted to Prof. J.L. Arias for the collaboration in SEM analysis and to G.B. Galland for the ^{13}C NMR analysis.

References

[1] Van Reis R, Zydney A. Curr Opin Biotechnol 2001;12:208–11.
[2] Girard B, Fukumoto LR. Crit Rev Biotechnol 2000;20:109–75.
[3] Borcherding H, Hicke HG, Jorcke D, Ulbricht M. Ann NY Acad Sci 2003; 984:470–9.
[4] Zeman LJ, Zydney AL. Microfiltration and ultrafiltration. New York: Marcel Dekker; 1996.
[5] Masuoka T, Hirasa O, Onishi M, Seita Y. US Patent 5,186,835; 1993.
[6] Mahmud H, Kumar A, Nrbaitz RM, Matsuura T. J Membr Sci 2002;209: 207–19.
[7] Matsuyama H, Berghmans S, Lloyd DR. J Membr Sci 1998;142:213–24.
[8] Castro AJ. US Patent 4,247,498; 1981.
[9] Lloyd DR, Kim S, Kinzer E. J Membr Sci 1991;64:1–11.
[10] Matsuyama H, Kudary S, Kiyofuji H, Kitamura Y. J Appl Polym Sci 2000;76:1028–36.
[11] Kim SS, Lloyd DR. J Membr Sci 1991;64:13.
[12] Hiat WC, Vitzthum GH, Wagener KB, Gerlach K, Josefiak C. Microporous membrane via upper critical temperatura phase separation. Material science of synthetic membranes, ACS symposium series 269, Washington, DC 1985.
[13] Kaminski W, Hähnsen H, Külper K, Woldt R. US Patent 4,542,199; 1985.
[14] Miller SA, Bercaw JE. Organometallics 2002;21:934–45.
[15] Quijada R, Guevara JL, Yazdani-Pedram M, Gallan GB, Ribeiro D. Polym Bull 2002;49:273–80.
[16] Kim DW, Yoshino K. J Phys D: Appl Phys 2000;33:464–71.
[17] Choi D, White JL. Polym Eng Sci 2002;42:1642–56.
[18] Shen Y, Wu P. J Phys Chem B 2003;107:4224–6.
[19] Jones TD, Chaffin KA, Bates FS. Macromolecules 2002;35:5061–8.
[20] Guevara JL. Dissertation. Chile: Chile University; 2004.
[21] Guevara JL, Quijada R, Saavedra P, Palza H, Galland GB. Bol Soc Chil Quim 2002;47:81–90.
[22] McGuire KS. Dissertation. Austin: The University of Texas; 1995.
[23] Atkinson PM, Lloyd DR. J Membr Sci 2000;175:225–38.
[24] Yave W, Quijada R, Serafini D, Lloyd DR. J Membr Sci 2005;263: 146–53.
[25] Yave W, Quijada R, Serafini D, Lloyd DR. J Membr Sci 2005;264:154–9.
[26] Atkinson PM. Dissertation. Austin: University of Texas; 1999.
[27] Matsuyama H, Berghamans S, Lloyd DR. Polymer 1999;40:2289–301.
[28] Lloyd DR, Barlow JW. New membrane materials and processes for separation. AlChE symposium series. vol. 84. New York: American Institute of Chemical Engineering; 1988 [p. 28–41].
[29] Atkinson PM, Lloyd DR. J Membr Sci 2000;171:1–18.
[30] Matsuyama H, Teramoto M, Kudary S, Kitamura Y. J Appl Polym Sci 2001;82:169–77.
[31] McGuire KS, Laxminarayan A, Martula DS, Lloyd DR. J Colloid Interface Sci 1996;182:46–58.
[32] Laxminarayan A, McGuire KS, Kim SS, Lloyd DR. Polymer 1994;35: 3060–8.
[33] McGuire KS, Laxminarayan A, Lloyd DR. Polymer 1995;36:4951–60.
[34] Erbil HY, Demirel AL, Ava Y, Mert O. Science 2003;299:1377–80.
[35] Caplan MR, Chiang CY, Lloyd DR, Yen LY. J Membr Sci 1997;130: 219–37.
[36] Matsuyama H, Yuasa M, Kitamura Y, Teramoto M, Lloyd DR. J Membr Sci 2000;179:91–100.
[37] Turner-Jones A. Polymer 1971;12:487.
[38] Natta G, Corradini P, Ganis P. Macromol Chem 1960;39:238.
[39] Lotz B, Lovinger AJ, Casi RE. Macromolecules 1988;21:2375.
[40] Lovinger AJ, Lotz B, Davis DD, Padden Jr JF. Macromolecules 1993;26: 3494–503.
[41] De Rosa C, Corradini P. Macromolecules 1993;26:5711.
[42] De Rosa C, Auriemma F, Corradini P. Macromolecules 1996;29:7452–9.

[43] Rodríguez-Arnold J, Bu ZZ, Cheng SZD. J Macromol Sci Rev Macromol Chem Phys 1995;C35:117–54.
[44] De Rosa C, Auriemma F, Vinti V. Macromolecules 1997;30: 4137–46.
[45] Mansel S, Pérez E, Benavente R, Pereña JM, Bello A, Röll W, et al. Macromol Chem Phys 1999;200:1292–7.
[46] Auriemma F, Ruiz de Ballesteros O, De Rosa O. Macromolecules 2001; 34:4485–91.
[47] Manual for Permporometer CFP-34RTG8A-X-6-L4, Porous Materials Inc., Ithaca, NY, USA; 2002.
[48] Kesting RE. Synthetic polymeric membranes. A structural perspective. Irvine, California: Wiley; 1985.
[49] Nielsen LE, Landel RF. Mechanical properties of polymers and composites. 2nd ed. New York: Marcel Dekker; 1994.
[50] Yoshino K, Demura T, Kawahigashi M, Miyashita Y, Kurahashi K, Matsuda Y. Electrical Eng Jpn 2004;146:18–26.